Separation Science and Technology
Publication details, including instructions for authors and subscription information:
http://www.informaworld.com/smpp/title~content=t713708471

Filtration with Sedimentation: Application of Kynchs Theorems

R. Font[a]; A. Hernández[a]
[a] DEPARTAMENTO DE INGENIERÍA QUÍMICA, UNIVERSIDAD DE ALICANTE, ALICANTE, SPAIN

Online publication date: 17 January 2000

To cite this Article Font, R. and Hernández, A.(2000) 'Filtration with Sedimentation: Application of Kynchs Theorems', Separation Science and Technology, 35: 2, 183 — 210
To link to this Article: DOI: 10.1081/SS-100100151
URL: http://dx.doi.org/10.1081/SS-100100151

SEPARATION SCIENCE AND TECHNOLOGY, **35**(2), pp. 183–210, 2000

Filtration with Sedimentation: Application of Kynch's Theorems

R. FONT* and A. HERNÁNDEZ
DEPARTAMENTO DE INGENIERÍA QUÍMICA
UNIVERSIDAD DE ALICANTE
APARTADO 99, ALICANTE, SPAIN

ABSTRACT

Filtration at moderate rates on upward-facing horizontal surfaces is accompanied by sedimentation. Kynch theorems developed for sedimentation in the noncompression range can be adapted to explaine the evolution of the cake surface and the filtrate volume with time. The different relationships obtained have been tested with filtration + sedimentation runs and filtration without sedimentation runs carried out with calcium carbonate suspensions at moderate pressure differences from 17 to 97 mmHg. The differences between the average specific resistance observed at the different runs can be satisfactorily explained by the fundamentals of the theory.

INTRODUCTION

The study of sedimentation and filtration of complex, often flocculated, dispersions can be considered by straightforward conservation equations and constitutive equations relating fluxes to driving forces through permeability/hindered settling coefficients and compressive yield stresses by partial differential equations that must be solved numerically (1–5).

Other researchers have considered the solutions of derivative equations using algebraic balances by considering characteristic lines and average properties such as average specific resistance to obtain interesting relations which are also useful for the design of thickeners and filters (6–10).

In some solid–fluid filtration on horizontal surfaces at moderate filtration rates, the process of sedimentation above the cake results in a variation of the

* To whom correspondence should be addressed. E-mail: rafael.font@ua.es

filtration rate. Tiller et al. (11) recently presented an interesting paper on filtration with sedimentation. They recognized in their conclusions that conventional theory can lead to substantial errors, and they considered the convenience of theoretical analysis for explaining the process of filtration with sedimentation.

Alicante University has been working with the fundamentals of sedimentation (12–14). The theory developed for compressible suspensions is adapted and tested in this paper with the process of filtration with sedimentation.

Conventional filtration theory is based on a two-resistance (cake + supporting medium) model and has been widely considered by Ruth (16), Tiller and Cooper (17), Tiller and Shirato (18), Holdich (19, 20), Stamatakis and Tien (21), Wells and Dick (22), Landman et al. (3), and Sørensen et al (23, 24). A summary of the main previous aspects considered in this paper are included in the reference by Tiller et al. (11).

Two ranges of solids concentration can be distinguished in the sedimentation of compressible suspensions: the noncompression or hindered settling zone where the aggregates or flocs descend separately although there is hindering among themselves, and the compression zone where the structure of the separated aggregates has disappeared and a matrix of solids has been formed. Analysis of the sedimentation is done by considering characteristic lines (constant solids concentration and constant settling rate) in the noncompression zone and lines of constant solids concentration (with non-constant settling rate) in the compression zone or sediment (6–9, 12, 13).

In a batch experiment of filtration with sedimentation, in accordance with the analysis done by Tiller et al. (11), the zones that can be distinguished can be observed in Fig. 1.

The variations observed vs time correspond to the liquid height H, the suspension or slurry height H_s, and the sediment or cake height L. The volume filtrate by unit of cross section equals $H_0 - H$, where H_0 is the initial liquid height. The characteristic lines can emerge from the bottom or from the cake surface.

Bockstal et al. (25) analyzed this phenomenon when the height of the suspension H_s descends with respect to the height of the liquid H with constant rate. The general treatment presented in the study developed can be applied to any situation.

EXPERIMENTAL

Calcium carbonate suspensions were used for testing the procedure proposed in this paper (density 2648 kg/m^3; cumulative weight fraction: 0.5 μm, 3.9%; 1.0 μm, 4.5%; 2.0 μm, 10.2%; 4.0 μm, 27.4%; 6.0 μm, 45.6%; 8.0 μm,

MARCEL DEKKER, INC.
270 Madison Avenue, New York, New York 10016

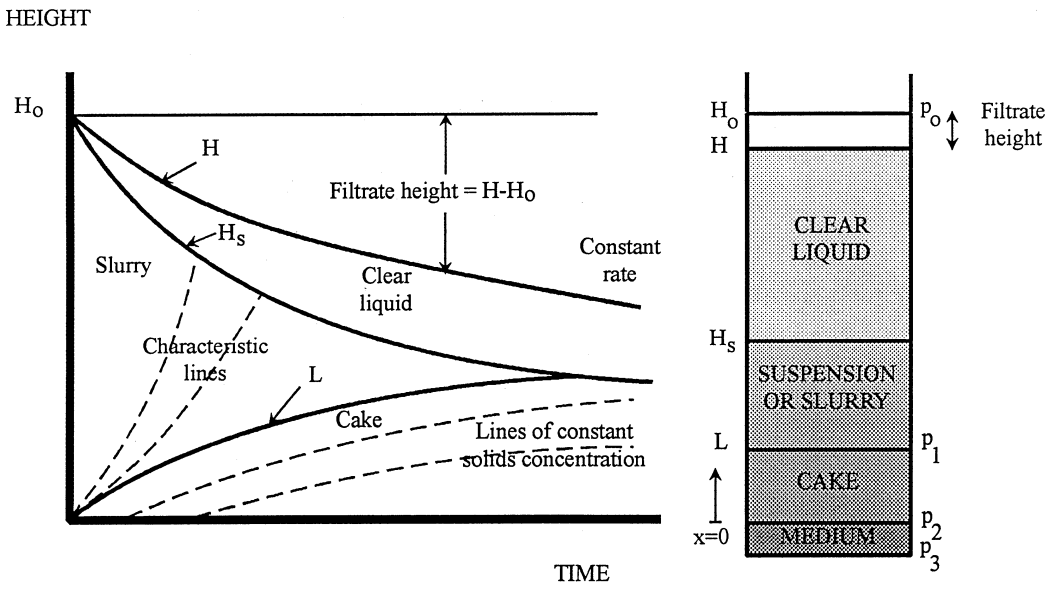

FIG. 1 Variation of discontinuities vs time in a filtration with sedimentation run.

59.1%; 10.0 μm, 69.1%; 15.0 μm, 84.8%; 20.0 μm, 93.3%; 25 μm, 97.6%; 30.0 μm, 99.4%; 40.0 μm, 100%; the mean surface diameter equals 4.3 μm).

Runs were carried out with a constant section glass filter, where the supporting medium was a sintered glass slab with filter paper (inside diameter 0.0915 m; height 0.1 m). In order to be able to see the location of the sediment, potassium permanganate to a maximum of 0.1 wt% was added in all the runs. It had previously been tested that the presence of this colorant did not modify the filtration rate nor the descent of the liquid interface and suspension interface.

Some filtration runs were done without sedimentation above the cake. A stirrer was therefore placed in the upper part of the filter to move the suspension and avoid sedimentation. In this case the liquid height and the suspension height coincided. Due to the stirring, the cake surface was smoothly waved and the cake height could not be accurately determined.

The vacuum pressures used for performing the runs were between 17 and 97 mmHg.

The average solidosities or volume fractions of solids in the cakes were determined by weight (wet and dry cake) and by a volume balance (initial suspension height, final cake height).

A sedimentation batch test in a glass cylinder was also done to compare the results (inside diameter 0.08 m; height 0.32 m).

All the runs were carried out at 25–27°C and with 25 wt% $CaCO_3$, which corresponds to an initial volume fraction of solids of 0.1115.

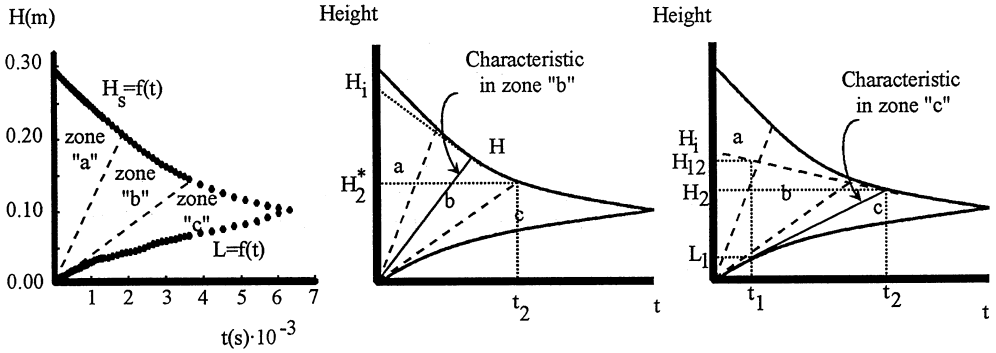

FIG. 2 Batch test of sedimentation: zones and notations.

EXPERIMENTAL RESULTS

Batch Sedimentation Test

Figure 2 shows the experimental results obtained in the batch sedimentation test carried out with initial volume fraction of solids $\phi_{s0} = 0.1115$. In this test the following zones can be drawn in the noncompression zone: zone "a" where the solids concentration is constant, zone "b" where the characteristic lines arise from the bottom, and zone "c" where the characteristic lines arise tangently from the sediment surface.

The critical or gel volume fraction of solids (limit between hindered settling zone and compression zone) can be calculated by the relation

$$\varepsilon_{s1} = \phi_{s0} H_0 / H_2^* \tag{1}$$

where H_2^* is the intercept height of the tangent to the sediment at the origin with the upper discontinuity (12) and H_0 is the initial height of suspension.

Depending on the tangent drawn to the sediment at the origin, the value of the critical or gel solidosity can oscillate in a certain interval of solids concentration. By correlating the experimental data $H = f(t)$ and $L = f(t)$ by polynomial equations, differentiating $L = f(t)$ to obtain the slope at the origin, and calculating the intercept between the tangent drawn at the origin and the upper discontinuity, the value of ε_{s1} equals 0.215. By considering the initial rising of the sediment for the first 500 seconds as linear vs time, and applying Eq. (1), the critical volume fraction of solids equals 0.270. This means that the critical solidosity is between 0.215 and 0.270, probably closer to 0.215, but with a small increase of solids pressure the solidosity of the sediment increases to 0.27.

For the initial solids concentration, the settling rate can be calculated from the slope of the straight line of the upper discontinuity for the first period (not considering the small initial portion that deviates from linearity as a conse-

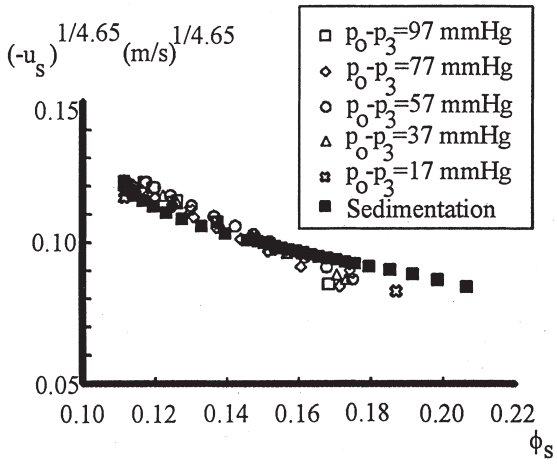

FIG. 3 Variation of (settling rate)$^{1/4.65}$ vs volume fraction of solids ϕ_s in the noncompression zone, considering the data of the sedimentation test and of filtration with sedimentation runs.

quence of the stirring; this initial portion is small for stable flocculated suspensions).

Considering the characteristic lines drawn in zones "b" and "c" (12), and applying the following equations:

For zone "b"

$$\phi_s = \phi_{s0} H_0 / H_i, \qquad (-u_s) = -dH/dt \tag{2}$$

For zone "c"

$$\phi_s = \frac{\phi_{s0} H_0}{H_{12} - L_1} \exp\left(-\int_0^{t_1} \frac{dt_1}{t_2 - t_1} \right), \qquad (-u_s) = -dH_2/dt_2 \tag{3}$$

the relation between the settling rate $(-u_s)$ (determined as $-dH/dt$ or $-dH_2/dt_2$) vs ϕ_s is obtained (the significance of some terms can be found in Fig. 2). Figure 3 shows the experimental variation obtained plotted as $(-u_s)^{1/4.65}$ vs ϕ_s. The values of $(-u_s)$ are the positive ones corresponding to the settling rate u_s which are negative in accordance with the positive semiaxis considered (in this paper the negative magnitudes are written between parentheses with the sign minus).

Filtration without Sedimentation Runs

Five runs were carried out at different pressure increments with stirring in the upper part of the filter. Figure 4 shows the experimental results for a test from which the evolution of the suspension height H_s and the cake surface L can be obtained.

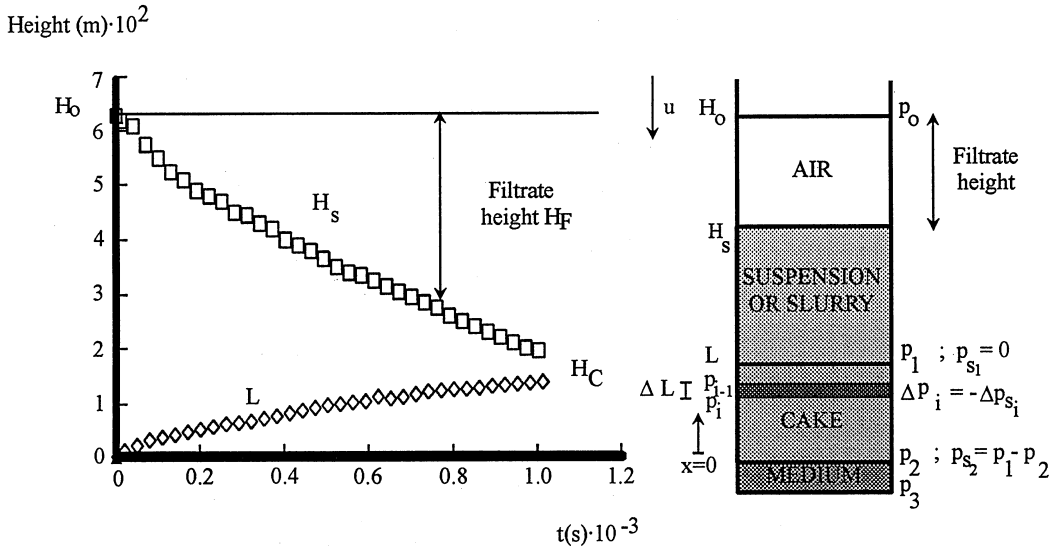

FIG. 4 Variation of the supernatant–suspension height H_s and the cake surface L vs time for a filtration without sedimentation run ($p_0 - p_3 = 57$ mmHg) and notations.

In order to compare the conventional theory of filtration without sedimentation with the theory of filtration with sedimentation presented in this paper in the following sections, the fundamentals of the conventional theory with some small corrections are briefly presented in Appendix 1.

The average volume fraction of solids $\varepsilon_{s,ave}$ of the cake can be calculated from the ratio M (wet cake mass/dry cake mass) by

$$\varepsilon_{s,ave} = \frac{\rho_s(M-1)}{\rho_s(M-1)+\rho} \tag{4}$$

where ρ_s is the solids density.

Another method for calculating $\varepsilon_{s,ave}$ when the sediment height can be determined is by the equation

$$\varepsilon_{s,ave} = \phi_{s0} H_0 / H_c \tag{5}$$

where H_c is the critical height of the cake when the upper interface intercepts the sediment interface.

It can be deduced at any time (see Appendix 1) that

$$A\frac{dt}{dV} = \frac{\mu\alpha_{s,ave}}{A(p_1-p_3)}W_s + \frac{\mu R_f}{p_1-p_3} \tag{6}$$

where $p_1 - p_3$ is the pressure loss through the cake and the supporting membrane, A is the cross area, V is the filtrate volume, t is the time, μ is the fluid viscosity, $\alpha_{s,ave}$ is the average specific resistance, and R_f is the membrane re-

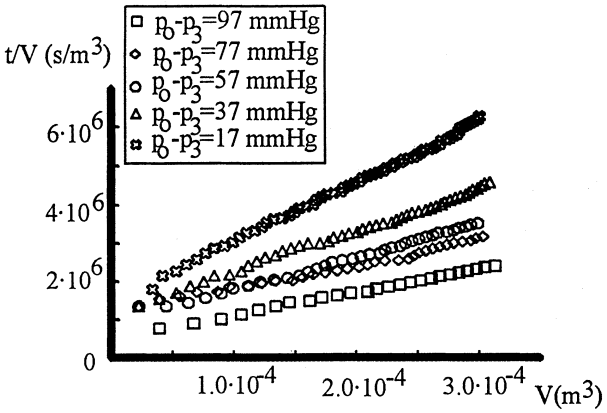

FIG. 5 Variation of the ratio t/V of the time to the filtrate volume vs the filtrate volume V for filtration without sedimentation runs.

sistance. The relation between the filtrate volume V and the time when $p_1 - p_3$ remains constant along the run is (see Appendix 1)

$$\frac{t}{V} = \frac{\mu\rho S_0 \alpha_{s,ave}}{2(1 - MS_0)A^2(p_1 - p_3)} V + \frac{\mu R_f}{A(p_1 - p_3)} \tag{7}$$

This equation is correct for incompressible cakes, but it can also be used for compressible cakes, as indicated in this paper. Landman et al. (3) deduced that when membrane resistance is negligible, the variation of t/V vs V for compressible cakes is linear, but the same conclusion can be obtained for incompressible cakes because in this case $\alpha_{s,ave}$ is constant because at any time the cake undergoes the same total pressure drop $p_1 - p_3$.

Figure 5 shows the variation of t/V vs V for the five runs carried out at different pressure increments where linear variations can be observed, excepting the first points. Considering only the second half of the points, where linearity is more clearly observed and where it is expected that the variations of $\alpha_{s,ave}$ and $\varepsilon_{s,ave}$ are small, the corresponding linear correlations and the values of $\alpha_{s,ave}$ and R_f were obtained.

Table 1 shows the experimental parameters corresponding for the five filtration without sedimentation runs:

- The vacuum carried out corresponds to "$p_0 - p_3$," but the real pressure differences across the cake "$p_1 - p_3$" are somewhat greater due to the weight of the suspension. An increment of 3 mmHg was considered to correspond to a mean suspension height of 3–4 cm.
- Values of R_f were calculated from ordinates at the origin in accordance with Eq. (7). A general tendency for it to increase with the pressure difference was observed (except for Run 5, due probably to the non-uniformity of the filter medium).

TABLE 1
Experimental Parameters for Filtration without Sedimentation Runs

Run	$p_0 - p_3$ mmHg	$p_1 - p_3$ mmHg	R_f (m^{-1}) $\times 10^{-10}$	$p_1 - p_2$ mmHg	M	$\varepsilon_{s,ave}$ by Eq. (15)	$\alpha_{s,ave}$ (m/kg) $\times 10^{-10}$
1	17.0	20.0	2.04	15.6	1.406	0.481	1.03
2	37.0	40.0	2.92	34.5	1.392	0.489	1.47
3	57.0	60.0	4.89	55.0	1.381	0.497	1.60
4	77.0	80.0	6.07	73.6	1.358	0.513	1.86
5	97.0	100.0	3.51	91.6	1.358	0.513	1.98

- The pressure losses "$p_1 - p_2$" throughout the cake are calculated by the equation

$$p_1 - p_2 = (p_1 - p_3) - \mu R_f (-u^+) \tag{8}$$

  by considering an average value of $(-u^+)$ corresponding to the second half of the points in Fig. 5.
- Values of $\varepsilon_{s,ave}$ were calculated by Eq. (4) by considering the values of M obtained from the wet mass and dry cake mass data (values of $\varepsilon_{s,ave}$ were not determined by Eq. 5 because the horizontal level of the cake surface was not uniform due to the stirring of the suspension above the cake).
- The specific resistance values $\alpha_{s,ave}$ were calculated from the slope of the correlation obtained (Fig. 5), in accordance with Eq. (7). As expected for compressible cakes, an increasing variation vs pressure difference can be observed.

Filtration Runs with Sedimentation

Five filtrations with sedimentation runs were also carried out at different pressure increments. Figure 6 shows the experimental values for a test in which the evolution of the liquid height H, the suspension height H_s and the cake height L can be observed.

Above the cake the solids descend with a velocity $(-u_s)$ which is the sum of two velocities: a) the filtration velocity $(-u^+)$, which is the average of the solids + liquid mixture in any section, and b) the real settling rate $(-u_s^{\#})$ of solids with respect to the mixture as a consequence of the sedimentation process of the solids at the hindered settling zone and where $(-u_s^{\#})$ is a function of only the solids concentration.

The relation between the settling rate $(-u_s^{\#})$ and the solids concentration can be calculated as in the batch testing of sedimentation if the filtrate height

MARCEL DEKKER, INC.
270 Madison Avenue, New York, New York 10016

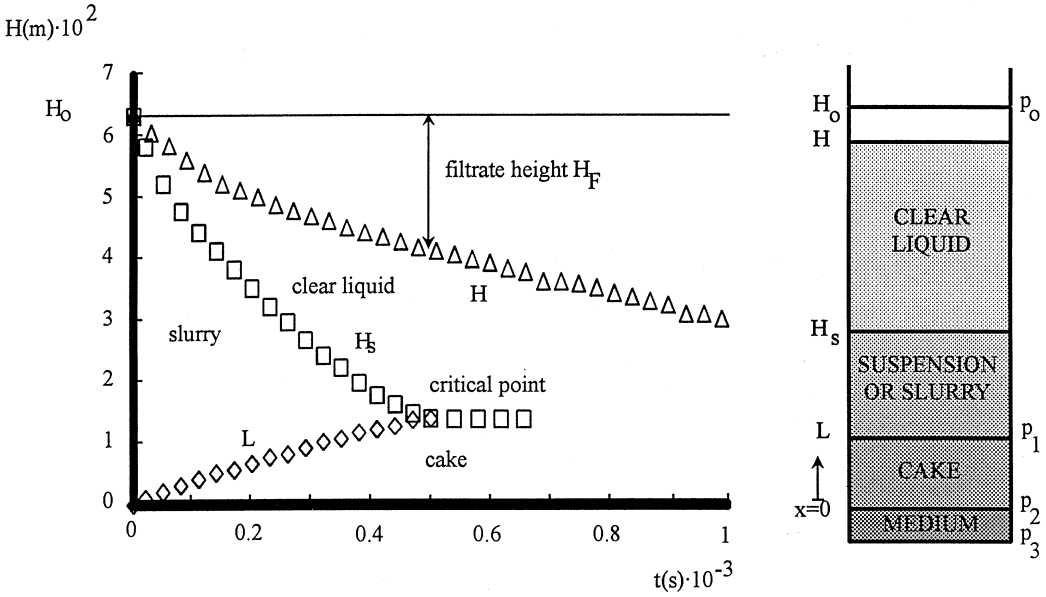

FIG. 6 Variation of the liquid height H, the supernatant–suspension height H_s, and the cake surface L vs time for a filtration with sedimentation run ($p_0 - p_3 = 57$ mmHg).

$(H_0 - H)$ is added to the suspension height H_s and to the cake height L to obtain the corresponding values of $H_s^{\#}$ and $L^{\#}$, as indicated in Fig. 7. With the curves $H_s^{\#} = f(t)$ and $L_s^{\#} = f(t)$, the relation $(-u_s^{\#}) = f(\phi_s)$ can be obtained in the same way as in batch testing of sedimentation. These applications are an important part of this paper; they are presented and discussed in Appendix 2 to clarify the discussion and methodology with the experimental results.

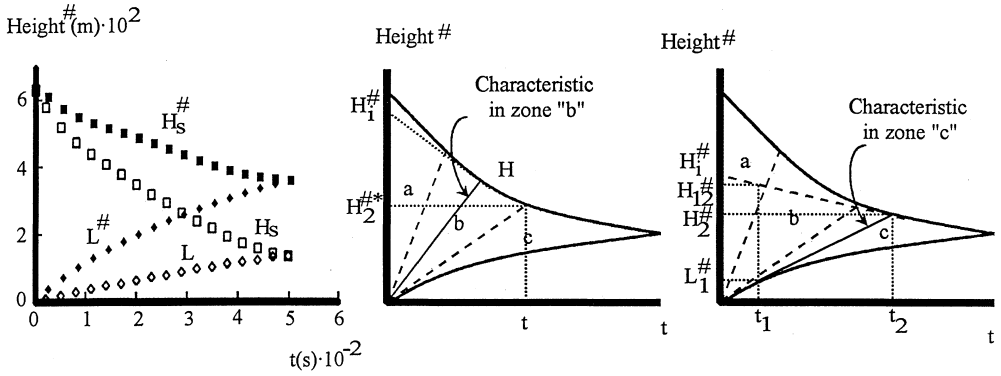

FIG. 7 Modified height–time diagram when adding the filtrate height $H_0 - H$ for a filtration with sedimentation run ($p_0 - p_3 = 57$ mmHg).

MARCEL DEKKER, INC.
270 Madison Avenue, New York, New York 10016

Deduction of the Relation between the Settling Rate ($-u_s^{\#}$) and the Volume Fraction of Solids

The settling rate corresponding to the initial solids concentration can be calculated from the slope of the straight line observed for the first few minutes (zone "a"). Considering the experimental data obtained with the calcium carbonate suspensions, there is an initial period of decreasing settling rate (also observed in batch runs of sedimentation), probably due to the initial stirring; this initial period has not been considered.

As a consequence of the adaptation of the Kynch theorems (Appendix 2), it is deduced that:

For zone "b"

$$\phi_s = \phi_{s0} H_0 / H_i^{\#}, \qquad (-u_s^{\#}) = -dH^{\#}/dt \tag{9}$$

Considering the experimental points shown in Fig. 7 and taking into account that the variation of the upper discontinuity is linear in the zone prior to the characteristic that arises tangently from the sediment surface, it is deduced that zone "b" coincides with zone "a" or is very thin.

For zone "c"

$$\phi_s = \frac{\phi_{s0} H_0}{H_{12}^{\#} - L_1^{\#}} \exp\left(- \int_0^{t_1} \frac{dt_1}{t_2 - t_1} \right), \qquad (-u_s^{\#}) = -dH_2^{\#}/dt_2 \tag{10}$$

From the modified $H_s^{\#} = f(t)$ and $L^{\#} = f(t)$ variations of the five runs, the series of $(-u_s^{\#})^{1/4.65}$ values obtained were plotted versus the corresponding values of volume fraction of solids, together with the data of batch testing in Fig. 3. They show the same general tendency of variation, and so corroborate the assumptions made.

In accordance with the Richardson and Zaki (26) relation and the methodology discussed in another paper (15), the relation $(-u_s) = f(\phi_s)$ was considered for all the points plotted in Fig. 3.

For $\phi_s < 0.16$, a linear variation of $(-u_s)^{1/4.65}$ vs ϕ_s was considered, so

$$(-u_s) = (-u_{s0})\,(1 - j\phi_s)^{1/4.65} = 2.70 \times 10^{-4}(1 - 2.7\phi_s)^{4.65}\ \text{m/s} \tag{11}$$

where the ratio "j" (aggregate volume/solids volume in an aggregate), known also as AVI (average volume index), takes the value of 2.7. By considering the value of $(-u_{s0})$ ($= 2.70 \times 10^{-4}$ m/s), the aggregate density ρ_a, calculated as $(\rho_s + (j - 1)\rho)/j$ ($= 1608$ kg/m^3), and the Stokes relation for creeping flow (Reynolds number < 0.2)

$$(-u_{s0}) = \frac{g d_a^2 (\rho_a - \rho)}{18\mu} \tag{12}$$

MARCEL DEKKER, INC.
270 Madison Avenue, New York, New York 10016

the aggregate diameter "d_a" calculated is 28 μm, which is greater than the mean particle size 4.3 μm, indicating the flocculent character of the suspension.

For $\phi_s > 0.16$, the data can be approximately correlated by the relation

$$(-u_s) = 3.76 \times 10^{-4} j^{-\frac{1}{3}}(1 - j\phi_s)^{4.65} \tag{13}$$

where

$$j = -5.403\phi_s + 3.578 \tag{14}$$

Deduction of the Critical or Gel Volume Fraction of Solids

Considering the first characteristic line which arises tangently to the cake in a $H^{\#}$–t plot, the critical or gel volume fraction of solids ε_{s1} can be calculated by the relation

$$\varepsilon_{s1} = \frac{\phi_{s0} H_0}{H_2^{\#*} - (-u_0{}^{+})t_2^*} \tag{15}$$

where $H_2^{\#*}$ and t_2^* correspond to the height and the time, respectively, at the intersection of the characteristic tangent to the cake surface at the origin in a $H^{\#}$–t plot, as indicated in Fig. 8. The value $(-u_0^+)$ corresponds to the initial superficial velocity of fluid through the supporting medium (that is, the initial filtration rate).

Appendix 3 shows the deduction of Eq. (15). By considering the experimental results of the five filtration with sedimentation runs, values ε_{s1} were

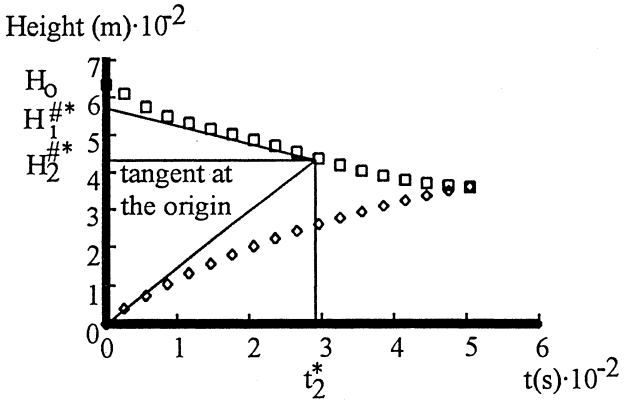

FIG. 8 Determination of the critical volume fraction of solids ε_{s1} from a run ($p_0 - p_3 = 57$ mmHg).

TABLE 2
Experimental Parameters for Filtration with Sedimentation Runs before the Critical Points

Run	$p_0 - p_3$ mmHg	ε_{s1}	$p_1 - p_3$ mmHg	R_f (m^{-1}) $\times 10^{-10}$	$p_1 - p_2$ mmHg	M	$\varepsilon_{s,ave}$ by Eq. (14)	$\varepsilon_{s,ave}$ by Eq. (15)	$\alpha_{s,ave}$ (m/kg) $\times 10^{-10}$
6	17.0	0.276	20.0	3.87	16.8	1.420	0.473	0.462	0.966
7	37.0	0.236	40.0	4.75	34.6	1.367	0.506	0.502	1.55
8	57.0	0.367	60.0	4.06	49.3	1.351	0.518	0.503	1.68
9	77.0	0.346	80.0	4.90	62.9	1.361	0.511	0.490	1.89
10	97.0	0.331	100.0	6.27	82.4	1.340	0.525	0.520	1.88

calculated, and they are presented in Table 2. It can be observed that the apparent critical volume fractions of solids are larger than the lowest limit 0.215 and close to the 0.215–0.270 range determined from the batch sedimentation test. It is logical that the apparent values deduced from the filtration with sedimentation runs are larger than the real one ε_{s1}, probably because of the compression of the initial layers of cake as a consequence of the high liquid flow at the beginning of the tests (with very thin cakes and the available data, the solidosity would probably be close to 0.215).

Deduction of the Average Specific Resistance $\alpha_{s,ave}$ and the Average Solidosity $\varepsilon_{s,ave}$ with the Effective Solids Pressure

Equation (7) for filtration with sedimentation runs cannot be used because this equation considers a direct relationship between the solids mass in the cake and the filtration volume, and consequently another relation must be deduced.

Equation (6) continues to be valid. By taking into account an average specific resistance $\alpha_{s,ave}$ as approximately constant in the integration, it can be deduced that

$$A\frac{dt}{dV} = \frac{\mu\alpha_{s,ave}}{A(p_1 - p_3)}W_s + \frac{\mu R_f}{p_1 - p_3} \tag{16}$$

and separating variables and integrating

$$A\int_0^t dt = At$$

$$= \frac{\mu\alpha_{s,ave}}{A(p_1 - p_3)}\int_0^v W_s dV + \frac{\mu R_f}{p_1 - p_3}V \tag{17}$$

MARCEL DEKKER, INC.
270 Madison Avenue, New York, New York 10016

and

$$\frac{t}{V} = \frac{\mu\alpha_{s,ave}}{A(p_1 - p_3)V}\int_0^v W_s dV + \frac{\mu R_f}{p_1 - p_3} \tag{18}$$

If t/V values are plotted vs $(1/V)\int_0^v W_s dV$, a linear variation is obtained when $\alpha_{s,ave}$ and $\varepsilon_{s,ave}$ become approximately constant. By considering only the points of the linear variation (not considering the first points), it can be seen that the parameters corresponding to the slope and the ordinate at the origin are exactly the same as those deduced from the differential Eq. (16). Appendix 4 shows the deduction of the relation for calculating W_s/A from the $H^{\#}$–t plot. This relation is

$$\frac{W_s}{A} = \phi_{s0}H_0\rho_s\left\{1 - \exp\left[-\int_0^{t_1}\frac{1}{t_2 - t_1}\,dt_1\right]\right\} \tag{19}$$

From the variation of W_s and V vs time, the values of $(1/V)\int_0^v W_s dV$ can be calculated. Figure 9 shows the variations of "t/V" vs $(1/V)\int_0^v W_s dV$ for the five filtration with sedimentation runs showing linear variations, especially in the second part of the run, where it is expected that the variations of $\alpha_{s,ave}$ and $\varepsilon_{s,ave}$ are small. The corresponding linear correlations were obtained by considering only the second part of the points.

Table 3 shows the experimental parameters corresponding to the five filtration with sedimentation runs:

- Values of "$p_1 - p_3$" are somewhat greater than of "$p_0 - p_3$" due to the weight of the suspension (an increment of 3 mmHg was considered, corresponding to a suspension height of 3–4 cm).

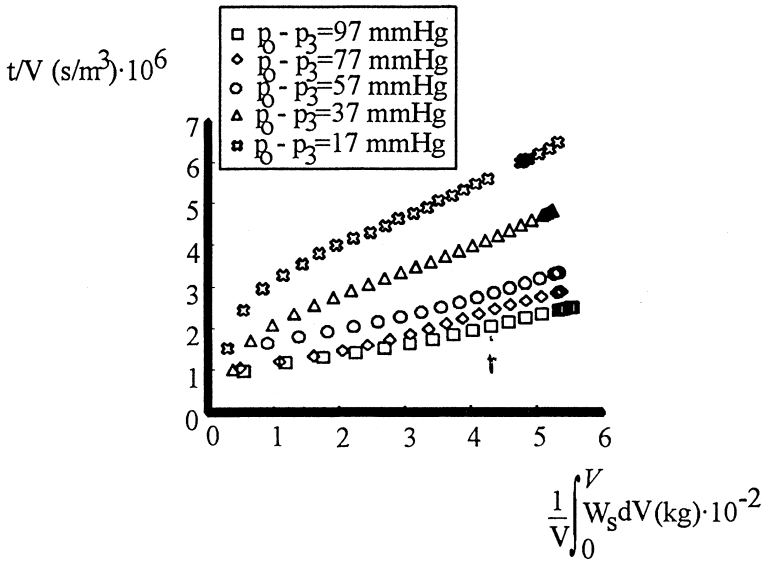

FIG. 9 Variation of ratio t/V of the time to the filtrate volume vs $(1/V)\int_0^V W_s dV$ for the five filtrations with sedimentation runs.

TABLE 3
Experimental Parameters for Filtration with Sedimentation Runs after the Critical Points

Run	$p_0 - p_3$ mmHg	$p_1 - p_3$ mmHg	R_f $(m^{-1}) \times 10^{-10}$	$(-u^+)$ $(m/s) \times 10^5$	$p_1 - p_2$ mmHg	$\alpha^*_{s,ave}$ $(m/kg) \times 10^{-10}$
6	17.0	20.0	3.87	0.950	17.2	1.30
7	37.0	40.0	4.75	1.43	35.0	1.75
8	57.0	60.0	4.06	2.20	53.3	1.74
9	77.0	80.0	4.90	2.36	71.4	2.16
10	97.0	100.0	6.27	2.86	86.6	2.17

- Values of R_f were calculated from the linear correlations in accordance with Eq. (18) (ordinates at the origin), these values are similar and have the same variation tendency as those obtained with filtration without sedimentation runs.
- The pressure losses "$p_1 - p_2$" throughout the cake are calculated by Eq. (8), considering an average value of $(-u^+)$ in the second part of the points (Fig. 9).
- Experimental values M and values $\varepsilon_{s,ave}$ calculated by Eqs. (4) and (5) are also presented. It can be observed that the values of average solidosity are similar.
- The average specific resistance values $\alpha_{s,ave}$ were calculated from the slope in the linear correlations obtained (Fig. 9).

Considering the filtrate rates, which are constant from the critical points (intercepts of the cake surface height with the suspension height), the values of the specific resistances for the pressure loss "$p_1 - p_2$" can be calculated from the corresponding equations by considering only the permeation of the fluid throughout the cake (considering Eq. A9 in Appendix 1 to have the constant value $(-u^+)$ and known values of μ and W_s/A; the values of "$p_1 - p_2$" are calculated by Eq. 8 by taking into account the values R_f deduced previously). Note that in this case the values of the specific resistances correspond to the parameters $\alpha^*_{s,ave}$ without movement of solids inside the cake (defined in Eq. A8 in Appendix 1). Table 3 also shows the operating parameters and the values of $\alpha^*_{s,ave}$.

Figure 10 shows the variation of log $\alpha_{s,ave}$ vs log p_s for the different determinations (the effective solids pressure p_s throughout the cake equals the liquid pressure loss "$p_1 - p_2$"). It can be observed that the relations $\alpha_{s,ave} = f(p_s)$ for filtration with or without sedimentation are similar as a consequence of the fact that the values of J are probably also close, whereas the values of the specific resistance are higher (in some cases up to 10–15%) than the corresponding ones for the other processes for filtration without sedimentation after the

MARCEL DEKKER, INC.
270 Madison Avenue, New York, New York 10016

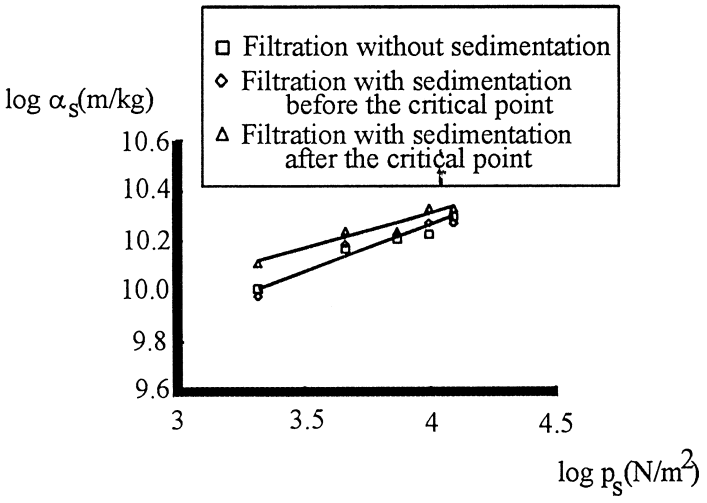

FIG. 10 Variation of the average specific resistance $\alpha_{s,ave}$ vs the effective solids pressure p_s.

critical point (percolation), indicating the small but significant influence of the parameter J.

From the correlation of the values obtained from the filtration with sedimentation runs (prior to the critical point) and the filtration without sedimentation runs, it is deduced that

$$\alpha_{s,ave}\,(\text{m/kg}) = 5.73 \times 10^8\, p_s^{0.377} \qquad (p_s \text{ in N/m}^2) \tag{20}$$

for $2{,}300 < p_s < 11{,}500$ N/m^2

Considering the experimental values for the 10 runs, when all the solids are in the cake, the following relation is obtained:

$$\varepsilon_{s,ave} = 0.3884 p_s^{0.0451} \qquad (p_s \text{ in N/m}^2) \tag{21}$$

for $2{,}300 < p_s < 11{,}500$ N/m^2

From the experimental data of filtration with or without sedimentation, the relationships between the local effective solids pressure, the permeability or the specific resistance, and the volume fraction of solids can be obtained. A computation program involving the previous relationships has been developed, and good simulation of all the runs was obtained, but this will be presented in another paper.

CONCLUSIONS

In a filtration batch process with sedimentation formed on the cake along the run, it is possible to apply the fundamentals developed for the sedimentation batch test if some modifications are included. By adding the variation of the filtrate height to the variation of the suspension–supernatant interface

height and to the cake surface height, the Kynch theorems can be applied to the new plot with the possibility of deducing the following relations and parameters: the relationship between the settling rate and the solids concentration, the apparent critical or gel solids concentration, the filter medium resistance, the solidosity, and the average specific resistance of the cake formed.

The fundamentals of the filtration with sedimentation run are tested by considering the similarity of some relations deduced from the different runs and by comparing them with some filtration without sedimentation tests.

From a batch test of filtration with sedimentation and by comparing the filtration process prior to and after the critical points, it is possible to analyze the influence of movement of solids inside the cake on the average specific resistance.

APPENDIX 1

By considering many layers of solids inside a cake and assuming a Darcian liquid flow, the superficial fluid velocity u_i^+ with respect to the solids can be related by the equation

$$\begin{aligned}(-u_i^+) &= [(-u_i) - (-u_{si})](1 - \varepsilon_{si}) \\ &= \frac{k}{\mu}\frac{dp_i^+}{dL_i} \\ &= \frac{1}{\mu}\frac{dp_i^+}{dR_i} \\ &= \frac{1}{\mu\alpha_{si}}\frac{dp_i^+}{d(W_{si}/A)}\end{aligned} \tag{A1}$$

where "$d(W_{si}/A)$" is the solids mass per unit of cross area corresponding to the layer with thickness "dL_i" or "dx," "u_i" is the fluid velocity, and "p_i^+" is the manometric pressure which equals "$p_i + \rho g x_i$" (in cakes the variation of "p" is much greater than "$\rho g x$," and consequently $p_i^+ \cong p_i$).

The superficial velocity defined for the filter medium or membrane filter is

$$(-u^+) = \frac{d(V/A)}{dt} = \frac{d(H_0 - H_S)}{dt} = \frac{dH_F}{dt} = \frac{p_2 - p_3}{\mu R_f} \tag{A2}$$

From a volume balance between a layer and the filter medium, it can be deduced that

$$(-u^+)A = (-u_i)A(1 - \varepsilon_{si}) + (-u_{si})\varepsilon_{si}A \tag{A3}$$

MARCEL DEKKER, INC.
270 Madison Avenue, New York, New York 10016

and consequently from the previous equation and Eq. (A1)

$$\begin{aligned}(-u_i^+) &= [(-u) - (-u_{si})](1 - \varepsilon_{si}) \\ &= (-u^+) - (-u_{si})\end{aligned} \tag{A4}$$

Equation (A1) can be written considering that $dp \cong dp^+ \cong -dp_s$ (deduced from a momentum balance, neglecting the small effect of the weight of the solids), where p_s is the effective pressure transmitted by the solids, so

$$(-u^+)\frac{W_s}{A}\frac{(-u^+) - (-u_{si})}{(-u^+)}\,d(W_{si}/W_s) = \frac{dp_i}{\mu\alpha_{si}} = \frac{-dp_{si}}{\mu\alpha_{si}} \tag{A5}$$

where "W_s" is the total solids mass. Integrating between the boundaries of the cake

$$\begin{aligned}(-u^+)\frac{W_s}{A} &= \frac{1}{\displaystyle\int_0^1 \frac{(-u^+) - (-u_{si})}{(-u^+)}\,d(W_{si}/W_s)} \int_{p_1}^{p_2} \frac{dp_i^+}{\mu\alpha_{si}} \\ &= \frac{1}{\displaystyle\int_0^1 \frac{(-u^+) - (-u_{si})}{(-u^+)}\,d(W_{si}/W_s)} \int_{p_1-p_2}^{0} \frac{-dp_{si}}{\mu\alpha_{si}} \\ &= \frac{p_1 - p_2}{\mu\alpha_{s,ave}} \\ &= \int_{p_1-p_2}^{0} \frac{-dp_{si}}{\dfrac{(-u^+) - (-u_{si})}{(-u^+)}\,\mu\alpha_{si}}\end{aligned} \tag{A6}$$

The last term of Eq. (A6) can easily be deduced from the arrangement of the terms in Eq. (A5). Consequently

$$\begin{aligned}\frac{1}{\alpha_{s,ave}} &= \frac{1}{p_1 - p_2}\left[\int_0^{p_1-p_2} \frac{dp_{si}}{\alpha_{si}}\right]\left[\frac{1}{\displaystyle\int_0^1 \frac{(-u^+) - (-u_{si})}{(-u^+)}\,d(W_{si}/W_s)}\right] \\ &= \frac{1}{\alpha^*_{s,ave}J} \\ &= \frac{1}{p_1 - p_2}\left[\int_0^{p_1-p_2} \frac{dp_{si}}{\dfrac{(-u^+) - (-u_{si})}{(-u^+)}\,\alpha_{si}}\right]\end{aligned} \tag{A7}$$

where

$$\frac{1}{\alpha^*_{s,ave}} = \frac{1}{p_1 - p_2}\left[\int_0^{p_1-p_2} \frac{dp_{si}}{\alpha_{si}}\right] \tag{A8}$$

and

$$\begin{aligned} J &= \int_0^1 \frac{(-u^+) - (-u_{si})}{(-u^+)}\, d(W_{si}/W_s) \\ &= \int_0^1 \frac{(-u_i^+)}{(-u^+)}\, d(W_{si}/W_s) \end{aligned} \tag{A9}$$

The expression "J" is similar to that defined by Tiller and Shirato (18) and corresponds to a correction factor (less than 1) as a consequence of the solids movement.

From Eqs. (A6) and (16)

$$\begin{aligned} (-u^+) &= \frac{d(V/A)}{dt} \\ &= \frac{p_1 - p_2}{\mu\alpha_{s,ave}\dfrac{W_s}{A}} \\ &= \frac{p_2 - p_3}{\mu R_f} \\ &= \frac{p_1 - p_3}{\mu\alpha_{s,ave}\dfrac{W_s}{A} + \mu R_f} \end{aligned} \tag{A10}$$

Assuming that the average solidosity of the cake is approximately constant along the run; introducing Eq. (4) in Eq. (A10); and integrating between $t = 0$, $V = 0$ and $t = t$, $V = V$; the following equation is obtained:

$$\frac{t}{V} = \frac{\mu\rho S_0\alpha_{s,ave}}{2(1 - MS_0)A^2(p_1 - p_3)}\, V + \frac{\mu R_f}{A(p_1 - p_3)} \tag{A11}$$

APPENDIX 2

In this section the application of the Kynch theorems when the filtrate height H_F is added to an H–t plot to obtain an $H^{\#}$–t diagram is discussed. The filtrate rate $(-u^+)$ can be related to the filtrate height H_F as

$$(-u^+) = dH_F/dt \tag{A12}$$

or

$$H_F = \int_0^t (-u^+)dt \tag{A13}$$

A line with slope "m" in an H–t diagram has a slope $m^\#$ in an $H^\#$–t diagram, calculated as

$$\begin{aligned} m^\# &= \frac{dH^\#}{dt} \\ &= \frac{d(H + H_F)}{dt} \\ &= \frac{dH}{dt} + \frac{dH_F}{dt} \\ &= m + (-u^+) \end{aligned} \tag{A14}$$

1st Kynch Theorem

Following the same procedures presented by Fitch (8) for a sedimentation batch test, the velocity v of a discontinuity arising in an H–t diagram (corresponding to a filtration with sedimentation run) can be calculated from a material balance applied to any cross section as

$$v = -\frac{\Delta[\phi_s(-u_s)]}{\Delta\phi_s} \tag{A15}$$

where $(-u_s)$ is the downward solids velocity, i.e, the sum of the downward settling rate $(-u_s^\#)$ and the superficial filtrate rate defined for the membrane $(-u^+)$, so

$$(-u_s) = (-u_s^\#) + (-u^+) \tag{A16}$$

Note that the superficial velocity equals the filtrate volume per unit of cross section and time and also equals the solids + liquid mixture that goes downward per unit of cross section and time at any height.

From Eqs. (A15) and (A16)

$$\begin{aligned} v &= -\frac{\Delta[\phi_s(-u_s)]}{\Delta\phi_s} \\ &= -\frac{\Delta[\phi_s((-u_s^\#) + (-u^+))]}{\Delta\phi_s} \\ &= -\frac{\Delta[\phi_s(-u_s^\#)]}{\Delta\phi_s} - (-u^+) \end{aligned} \tag{A17}$$

or

$$\begin{aligned} \nu^{\#} &= \nu + (-u^{+}) \\ &= -\frac{\Delta[\phi_s(-u_s^{\#})]}{\Delta\phi_s} \end{aligned} \tag{A18}$$

This means that the rising velocity $\nu^{\#}$ of a discontinuity in an $H^{\#}$–t diagram equals the expression obtained in a batch sedimentation test, where $(-u_s^{\#})$ is the downward settling rate of solids with respect to the mixture. Note that if both solids concentrations of the two extremes of the discontinuity are inside the noncompression zone [$(-u_s^{\#})$ depends only on ϕ_s], the variation of the discontinuity height vs time can be a curve in an H–t diagram because $(-u^{+})$ can change with time, whereas the variation of the discontinuity height vs time in an $H^{\#}$–t diagram is linear although $(-u^{+})$ changes with time, in accordance with Eq. (A18).

2nd Kynch Theorem

Following the same procedures presented by Fitch (8), the rising velocity ν of a characteristic line in an H–t diagram can be calculated from a material balance applied to an elemental volume as

$$\nu = -d[\phi_s(-u_s)]/d\phi_s \tag{A19}$$

From Eqs. (A16) and (A19)

$$\begin{aligned} \nu &= -\frac{d[\phi_s(-u_s)]}{d\phi_s} \\ &= -\frac{d[\phi_s((-u_s^{\#}) + (-u^{+}))]}{d\phi_s} \\ &= -\frac{d[\phi_s(-u_s^{\#})]}{d\phi_s} - (-u^{+}) \end{aligned} \tag{A20}$$

or

$$\begin{aligned} \nu^{\#} &= \nu + (-u^{+}) \\ &= -\frac{d[\phi_s(-u_s^{\#})]}{d\phi_s} \end{aligned} \tag{A21}$$

This means that the arising velocity $\nu^{\#}$ of a characteristic line in an $H^{\#}$–t diagram equals the expression obtained in batch testing, where $(-u_s^{\#})$ is the downward settling rate of solids with respect to the mixture, that only depends on the ϕ_s. Consequently, characteristic lines are curved in an H–t dia-

MARCEL DEKKER, INC.
270 Madison Avenue, New York, New York 10016

gram because $(-u^+)$ changes with time, whereas they are linear in an $H^\#$–t diagram.

3rd Kynch Theorem

From Eqs. (A16) and (A14) it can be written that

$$\begin{aligned}(-u_s^\#) &= (-u_s) - (-u^+) \\ &= -\frac{dH}{dt} - \left(\frac{dH_F}{dt}\right) \\ &= -\frac{d(H + H_F)}{dt} \\ &= -\frac{dH^\#}{dt}\end{aligned} \tag{A22}$$

Consequently, considering the $H^\#$–t diagram (Fig. 7), the slope of the upper interface in zone "a" corresponds to the settling rate of the initial solids concentration.

A deduction similar to that presented by Fitch (8) is made in zone "b." By considering the characteristic line that arises from the origin, the volume of solids that crosses the characteristic line is equal to the total volume of solids, and considering Fig. 7

$$\begin{aligned}[(-u_s^\#) + v^\#]t\phi_s S &= \phi_{s0} H_0 S \\ &= \left[\frac{H_i^\# - H^\#}{t} + \frac{H^\#}{t}\right] t\phi_s S \\ &= H_i^\# \phi_s S\end{aligned} \tag{A23}$$

and

$$\phi_s = \phi_{s0} H_0 / H_i^\# \tag{A24}$$

This means that the relationship between the settling rate and the volume fraction of solids can be obtained by drawing many characteristic lines and relating the slope of the upper interface (settling rate) with the volume fraction of solids given by Eq. (A24), as occurs in batch testing.

Relationship between the Settling Rate and the Volume Fraction of Solids When the Characteristics Arise from the Cake Surface

The procedure is similar to that presented previously (9, 12) but considers the $H^\#$–t diagram. Figure 7 shows the rise of a characteristic line from the sed-

iment. The solids balance can be written at any moment as

$$\phi_{s0}H_0 = \int_0^{L_1} \varepsilon_s dx + \int_{L_1^\#}^{H_1^\#} \phi_s dx^\# \tag{A25}$$

Considering some relations from Fig. 7

$$\begin{aligned}\int_{L_1^\#}^{H_1^\#} \phi_s dx^\# &= \phi_{s2}[v^\# + (-u_{s2}^\#)](t_2 - t_1) \\ &= \phi_{s2}\left[\frac{H_2^\# - L_1^\#}{t_2 - t_1} + \frac{H_{12}^\# - H_2^\#}{t_2 - t_1}\right](t_2 - t_1) \\ &= \phi_{s2}(H_{12}^\# - L_1^\#)\end{aligned} \tag{A26}$$

Introducing Eq. (A26) in Eq. (A25):

$$\begin{aligned}\frac{d}{dt_1}\phi_{s0}H_0 &= 0 \\ &= \frac{d}{dt_1}\int_0^{L_1} \varepsilon_s dx + \frac{d}{dt_1}\int_{L_1^\#}^{H_1^\#} \phi_s dx^\# \\ &= \varepsilon_{s1}\frac{dL_1}{dt_1} + \int_0^{L_1} \frac{\partial \varepsilon_s}{\partial t_1} dx + \frac{d}{dt_1}[\phi_{s2}(H_{12}^\# - L_1^\#)] \\ &= \varepsilon_{s1}\frac{dL_1}{dt_1} + \varepsilon_{s1}(-u_{s1}) + \frac{d}{dt_1}[\phi_{s2}(H_{12}^\# - L_1^\#)] \\ &= \varepsilon_{s1}\left[\frac{dL_1}{dt_1} + (-u^+)\right] + \varepsilon_{s1}[(-u_{s1}) - (-u^+)] \\ &\quad + \frac{d}{dt_1}[\phi_{s2}(H_{12}^\# - L_1^\#)] \\ \therefore 0 &= \varepsilon_{s1}\frac{dL_1^\#}{dt_1} + \varepsilon_{s1}(-u_{s1}^\#) + \frac{d}{dt_1}[\phi_{s2}(H_{12}^\# - L_1^\#]\end{aligned} \tag{A27}$$

Note that in the previous equations the term $\int_0^{L_1} (\partial \varepsilon_s/\partial t_1)dx$ equals $\varepsilon_{s1}(-u_{s1})$ because this is the result of a material balance between the bottom and the top of a cake.

On the other hand, consider Eq. (A15) applied to the sediment surface:

$$\frac{dL_1^\#}{dt_1} = -\frac{\phi_{s2}(-u_{s2}^\#) - \varepsilon_{s1}(-u_{s1}^\#)}{\phi_{s2} - \varepsilon_{s1}} \tag{A28}$$

and

$$\phi_{s2}(-u^{\#}_{s2}) + \phi_{s2}\frac{dL^{\#}_1}{dt_1} = \varepsilon_{s1}\frac{dL^{\#}_1}{dt_1} + \varepsilon_{s1}(-u^{\#}_{s1}) \tag{A29}$$

From Eqs. (A27) and (A29) and considering Fig. 7:

$$\begin{aligned}\phi_{s2}(-u^{\#}_{s2}) + \phi_{s2}\frac{dL^{\#}_1}{dt_1} &= \frac{d}{dt_1}\left[\phi_{s2}(H^{\#}_{12} - L^{\#}_1)\right] \\ &= \phi_{s2}\frac{H^{\#}_{12} - H^{\#}_2}{t_2 - t_1} + \phi_{s2}\frac{H^{\#}_{12} - L^{\#}_1}{t_2 - t_1} \\ &= \phi_{s2}\frac{H^{\#}_{12} - L^{\#}_1}{t_2 - t_1} \\ &= (H^{\#}_{12} - L^{\#}_1)\frac{d\phi_{s2}}{dt_1} + \phi_{s2}\frac{d}{dt_1}\left[H^{\#}_{12} - L^{\#}_1\right]\end{aligned} \tag{A30}$$

Considering the last two terms of the previous equation and dividing by ($H^{\#}_{12} - L^{\#}_1$) ϕ_{s2}, rearranging the equation, and integrating:

$$-\int_{\phi_{s2}}^{\phi_{s2}}\frac{d\phi_{s2}}{\phi_{s2}} = \int_{H^{\#*}_i}^{H^{\#}_{12} - L^{\#}_1}\frac{d(H^{\#}_{12} - L^{\#}_1)}{H^{\#}_{12} - L^{\#}_1} + \int_0^{t_1}\frac{dt_1}{t_2 - t_1} \tag{A31}$$

where ϕ^{*}_{s2} corresponds to the characteristic line that rises tangently from the sediment, whose value of $H^{\#}_{12} - L^{\#}_1$ equals $H^{\#*}_i$ and taking into account that the characteristic line arises from the origin:

$$\phi^{*}_{s2} = \phi_{s0}H^{\#}_0/H^{\#*}_i \tag{A32}$$

Operating with Eq. (A31) and considering Eq. (A32):

$$\begin{aligned}\phi_{s2} &= \phi^{\#*}_{s2}\frac{H^{\#*}_i}{H^{\#}_{12} - L^{\#}_1}\exp\left[-\int_0^{t_1}\frac{dt_1}{t_2 - t_1}\right] \\ &= \frac{\phi_{s0}H_0}{H^{\#*}_i}\frac{H^{\#*}_i}{H^{\#}_{12} - L^{\#}_1}\exp\left[-\int_0^{t_1}\frac{dt_1}{t_2 - t_1}\right] \\ &= \frac{\phi_{s0}H_0}{H^{\#}_{12} - L^{\#}_1}\exp\left[-\int_0^{t_1}\frac{dt_1}{t_2 - t_1}\right]\end{aligned} \tag{A33}$$

which is the expression similar to that obtained in batch sedimentation testing. Consequently, in a modified $H^{\#}$–t diagram it is possible to correlate the values of ϕ_{s2} with the settling rate $dH^{\#}_2/dt_2$ obtained in the intercept on the supernatant–suspension discontinuity.

MARCEL DEKKER, INC.
270 Madison Avenue, New York, New York 10016

APPENDIX 3

By considering the normal *H–t* diagram (without modifications), and also that the sediment surface is a discontinuity, it can be written that

$$\begin{aligned}\left(\frac{dL}{dt}\right)_{t=0} &= -\frac{\Delta[\phi_s(-u_s)]}{\Delta\phi_s} \\ &= -\frac{\phi_s^*(-u_s^*) - \varepsilon_{s1}.0}{\phi_s^* - \varepsilon_{s1}} \\ &= \frac{\phi_s^*[(-u_s^{\#*}) + (-u_0^+)]}{\varepsilon_{s1} - \phi_s^*}\end{aligned} \tag{A34}$$

From Eq. (A32), and considering Eq. (A30) and Fig. 8:

$$\begin{aligned}\varepsilon_{s1} &= \frac{\phi_s^*\left[\left(\frac{dL}{dt}\right)_{t=0} + (-u_0^+) + (-u_s^{\#})\right]}{\left(\frac{dL}{dt}\right)_{t=0}} \\ &= \frac{\phi_{s0}H_0}{H_i^{\#*}} \frac{\left[\left(\frac{dL_1^{\#}}{dt}\right)_{t=0} + (-u_s^{\#})\right]}{\left(\frac{dL_1^{\#}}{dt}\right)_{t=0} - (-u_0^+)} \\ &= \frac{\phi_{s0}H_0}{H_i^{\#*}} \frac{\left[\frac{H_2^{\#*}}{t_2^*} + \frac{H_i^{\#*} - H_2^{\#*}}{t_2^*}\right]}{\frac{H_2^{\#*}}{t_2^*} - (-u_0^+)} \\ &= \frac{\phi_{s0}H_0^{\#*}}{H_2^{\#*} - (-u_0^+)t_2^*}\end{aligned} \tag{A35}$$

which is the expression for calculating ε_{s1}.

APPENDIX 4

The solids mass per unit of area that crosses the sediment can be calculated as

$$\frac{d\left(\frac{W_s}{A}\right)}{dt_1} = \rho_s\left[\phi_{s2}\left(-u_{s2} + \frac{dL_1}{dt_1}\right)\right]$$

MARCEL DEKKER, INC.
270 Madison Avenue, New York, New York 10016

$$= \rho_s \left[\phi_{s2} \left(-(u_{s2}^{\#} + (-u^+)) + \frac{dL_1^{\#}}{dt_1} + (u^+) \right) \right] \tag{A36}$$

$$= \rho_s \left[\phi_{s2} \left(-u_{s2}^{\#} + \frac{dL_1^{\#}}{dt_1} \right) \right]$$

Considering Eq. (A33) and some geometrical relations deduced from Fig. 7, Eq. (A36) becomes

$$d\left(\frac{W_s}{A}\right) = \rho_s \phi_{s2} \left(\frac{H_{12}^{\#} - H_2^{\#}}{t_2 - t_1} + \frac{H_2^{\#} - L_1^{\#}}{t_2 - t_1} \right) dt_1$$

$$= \rho_s \frac{\phi_{s0} H_0}{H_{12}^{\#} - L_1^{\#}} \left[\exp - \left(\int_0^{t_1} \frac{dt_1}{t_2 - t_1} \right) \right] \frac{H_{12}^{\#} - L_1^{\#}}{t_2 - t_1} dt_1 \tag{A37}$$

$$= \rho_s \frac{\phi_{s0} H_0}{t_2 - t_1} \left[\exp - \left(\int_0^{t_1} \frac{dt_1}{t_2 - t_1} \right) \right] dt_1$$

Integrating from $t = 0$:

$$\frac{W_s}{A} = \rho_s \phi_{s0} H_0 \left[1 - \exp \left(- \int_0^{t_1} \frac{dt_1}{t_2 - t_1} \right) \right] \tag{A38}$$

which is the relation for calculating the amount of solids inside the sediment.

SYMBOLS

A	cross section of the filter (m^2)
AVI	average volume index (aggregate volume/solids volume ration in an aggregate)
d_a	aggregate diameter (m or μm)
g	gravity acceleration (m/s^2)
H	liquid height (m)
H_F	filtrate height (filtrate volume per unit of cross section) (m)
H_i	intercept of the tangent to the suspension–supernatant interface on the x-axis in zone "b" (m)
H_0	initial height (m)
H_s	slurry or suspension height (m)
$H_i^{\#}$	intercept of the tangent to the suspension–supernatant interface on the x-axis in zone "b" in the modified diagram (Fig. 7) (m)
H_{12}	intersection height of the tangent at (t_2, H_2) with the vertical line at t_1 (m)
$H_{12}^{\#}$	intersection height of the tangent at (t_2, $H_2^{\#}$) with the vertical line at t_1 in the modified diagram (Fig. 7) (m)

H_2	suspension height at time t_2 (m)
H_2^*	intercept height of the tangent to sediment or cake at the origin with the suspension–supernatant height (m)
$H_2^{\#*}$	intercept height of the tangent to sediment or cake at the origin with the suspension–supernatant height in the modified height–time diagram (Fig. 7) (m)
$H_2^{\#}$	suspension height at time t_2 in the modified diagram (Fig. 7) (m)
H_c	critical height when the suspension intercepts with the sediment (m)
$H_s^{\#}$	suspension height in the modified height–time diagram (Fig. 7) (m)
j	aggregate volume/solids volume ration in an aggregate (equals AVI)
J	correction factor given by Eq. (A9) (dimensionless)
L	sediment height (m)
L_1	sediment or cake height at time t_1 (m)
$L_1^{\#}$	cake height at time t_1 in the modified diagram (Fig. 7)
M	wet cake mass/dry cake ratio
p	liquid pressure (N/m^2 or mmHg)
p^+	manometric or dynamic pressure (N/m^2)
p_s	effective solids pressure (N/m^2 or mmHg)
R	flow resistance (m^{-1})
R_f	medium filter resistance (m^{-1})
S_0	initial mass fraction of solids in the suspension (dimensionless)
t	time(s)
t_1	time at which the characteristic line of zone "c" arises tangently from the sediment(s)
t_2	time at the intersection of the characteristic of zone "c" with the suspension–supernatant interface(s)
t_2^*	time at which the characteristic line that rises tangently to the sediment curve and from the bottom intercept with the suspension–supernatant interface(s)
u_s	solids velocity (m/s)
u_{s1}	solids velocity at the top of the cake (m/s)
u_{si}	solids velocity at layer i (m/s)
u_i	liquid velocity at layer i (m/s)
u_{s0}	solids velocity at dilution infinity (settling rate of an aggregate) (m/s)
u^+	superficial liquid velocity at the filter medium (filtrate volume per unit of cross section and per unit of time) (m/s)
u_i^+	superficial velocity of solids with respect to liquid (m/s)
u_0^+	initial superficial velocity (m/s)
$u_s^{\#}$	settling rate of solids with respect to the suspension (m/s)

MARCEL DEKKER, INC.
270 Madison Avenue, New York, New York 10016

$u_{s2}^{\#}$ (settling rate of solids corresponding to the characteristic line that rises tangently to sediment (m/s)
V filtrate volume [equals $A(H_0 - H)$] (m^3)
W_s mass of solids in the cake (kg)
W_{si} mass corresponding to layer i inside the cake (kg)
x distance to the supporting medium (m)
$x^{\#}$ modified distance to the supporting medium ($= x + H_F$) (m)

Greek Letters

α_s specific resistance (m/kg)
α_{s1} specific resistance for the critical volume fraction of solids (m/kg)
$\alpha_{s,ave}$ average specific resistance of the cake (m/kg)
$\alpha_{s,ave}^{*}$ average specific resistance calculated by Eq. (A8)
ε_s volume fraction of solids or solidosity in the compression range (dimensionless)
ε_{si} volume fraction of solids of layer i inside the cake (dimensionless)
ε_{s1} critical or gel volume fraction of solids (dimensionless)
$\varepsilon_{s,ave}$ average solidosity of the cake (dimensionless)
μ liquid viscosity [kg/(m·s)]
ν arising velocity of a discontinuity or a characteristic in an H–t diagram (m/s)
$\nu^{\#}$ arising velocity of a discontinuity or a characteristic in an $H^{\#}$–t diagram (m/s)
ρ liquid density (kg/m^3)
ρ_a aggregate density (kg/m^3)
ρ_s solids density (kg/m^3)
ϕ_s volume fraction of solids in the noncompression zone (dimensionless)
ϕ_{s0} initial volume fraction of solids (dimensionless)
ϕ_{s2} volume fraction of solids corresponding to the characteristic that rises tangently to sediment (dimensionless)

REFERENCES

1. R. Buscall and L. R. White, *J. Chem. Soc., Faraday Trans. 1, 83,* 873 (1987).
2. K. A. Landman, L. R. White, and R. Buscall, *AIChE J., 34,* 239 (1988).
3. K. A. Landman, L. R. White, and M. Eberl, *Ibid., 41,* 1687 (1995).
4. M. D. Green, M. Eberl, and K. A. Landman, *Ibid., 42,* 2308 (1996).
5. M. D. Green and D. V. Boger, *Ind. Eng. Chem. Res., 36,* 4984 (1997).
6. B. Fitch, *AIChE J., 25,* 913 (1979).
7. B. Fitch, *Ibid., 29,* 940 (1983).
8. B. Fitch, *Ibid., 39,* 27 (1993).
9. F. M. Tiller, *Ibid., 27,* 823 (1981).

MARCEL DEKKER, INC.
270 Madison Avenue, New York, New York 10016

10. F. M. Tiller, *Chem. Eng. Prog.*, *49*, 467 (1953).
11. F. M. Tiller, N. B. Hsyung, and D. Z. Cong, *AIChE J.*, *41*, 1153 (1995).
12. R. Font, *Ibid.*, *34*, 229 (1988).
13. R. Font, *Ibid.*, *36*, 3 (1990).
14. R. Font, M. Perez, and C. Pastor, *Ind. Eng. Chem. Res.*, *33*, 2859 (1994).
15. R. Font, *Chem. Eng. Sci.*, *46*, 2473 (1991).
16. B. F. Ruth, *Ind. Eng. Chem.*, *38*, 564 (1946).
17. F. M. Tiller and H. Cooper, *AIChE J.*, *8*, 445 (1962).
18. F. M. Tiller and M. Shirato, *Ibid.*, *10*, 61 (1964).
19. R. Holdich, *Chem. Eng. Commun.*, *91*, 255 (1990).
20. R. Holdich, *Filtr. Sep.*, *31*, 825 (1994).
21. K. Stamatakis and C. Tien, *Chem. Eng. Sci.*, *46*, 1917 (1991).
22. S. A. Wells and R. I. Dick, *Adv. Filtr. Sep. Technol.*, *7*, 9 (1993).
23. P. B. Sørensen, P. Moldrup, and J. A. Hansen, *Chem. Eng. Sci.*, *51*, 967 (1996).
24. P. B. Sørensen, M. L. Agerbaek, and B. L. Sørensen, *Water Environ. Res.*, *68*, 1151 (1996).
25. F. Bockstal, L. Fourage, J. Hermia, and G. Rahier, *Filtr. Sep.*, *22*, 255 (1985).
26. J. F. Richardson and W. N. Zaki, *Trans. Inst. Chem. Eng.*, *32*, 35 (1954).

Received by editor August 30, 1998
First revision received May 1999
Second revision received June 1999

Request Permission or Order Reprints Instantly!